

Master in Photonics

MASTER THESIS WORK

**Progress towards a model for the propagation of
light in turbid media with irregular particles**

Miriam Perez Poncelas

Supervised by Dr./Prof. Santiago Royo Royo (CD6)

Presented on date 14th October 2021

Registered at

ETSETP Escola Tècnica Superior
d'Enginyeria de Telecomunicació de Barcelona

Progress towards a model for the propagation of light in turbid media with irregular particles

Miriam Perez Poncelas

CD6 (Centre for Sensors, Instruments and Systems Development), Universitat Politècnica de Catalunya, Rambla Sant Nebridi 10, Terrassa 08222, Spain

E-mail: miriam.perez.poncelas@estudiantat.upc.edu

Abstract. Literature on the propagation of light in turbid media has been thoroughly explored, so an existing visible radiometric propagation model based on Mie theory is improved, and it implies a progress towards a model for the propagation of light in turbid media with irregular particles. Radiation fog, biomass burning, and transported desert dust, have been characterized, and phase function, asymmetry parameter (g), single scattering albedo (SSA) and radiative transfer have been evaluated. According to the results obtained, refractive index, particle density, size distribution (which appeared to fit a log-normal), g , and SSA, have proved to be key parameters in the development of the radiometric calculation. For future work, the implementation of a method capable of reproducing the aerosol optical properties of non-irregular particles (e.g., T-matrix method) is encouraged as well as the experimental validation of this model.

Keywords: turbid media, radiative transfer, Mie theory, irregular particles

1. Introduction

Turbid media scatters and/or absorbs electromagnetic radiation at visible frequencies, thus observation and simulation of its characteristics contribute to a better understanding of the phenomena and to adapt technical solutions against visibility reduction in fields such as biology (e.g. health diagnostics), transports (e.g. plane landing) or communications (e.g. terrestrial free space optical communications, also known as FSO), among others. Notwithstanding, imaging through turbid media is a huge challenge.

In particular, our interest focuses solely on the improvement of imaging in the visible range during fog, wildfires or dust clouds episodes that take place in the planetary boundary layer (PBL), which represents the lowest part of the atmosphere, ranging anywhere between 100 and 2000 m above the surface of the ground [1].

The aim of this Master Thesis is to improve an existent radiometric model developed in C++, based on Mie theory and Monte Carlo method as well as to propose some improvements to be implemented in the future.

2. State of the art

Each experiment conducted in a turbid environment is unique. This happens because the nature of aerosols and meteorological conditions are in time unique as well, such as their components and the proportion in which they are manifested, their size, their shape, their particle density, their geographical location, their lifetime (i.e., time remaining in the atmosphere before they hit the ground), the humidity in the environment... [1] and consequently the aerosol optical properties derived may be altered. Thus, this prevents us from generating a global radiometric model.

2.1. Effects of nonsphericity on the aerosol optical properties

The aerosol optical properties of interest for modelling propagation are the extinction, scattering, and absorption coefficients and efficiencies (μ_{ext} , μ_{sca} , μ_{abs} , Q_{ext} , Q_{sca} , and Q_{abs} , respectively), the single scattering albedo (SSA), the phase function, and the asymmetry parameter (g) [2]. It should be noted that the statistical distribution of sizes of the particles is a key parameter in the calculation of the aerosol optical properties and eventually in the radiometric results.

Mie theory is commonly used in models to describe these aerosol optical properties, given the size range of aerosol particles, which is comparable to the wavelength in the visible, and assuming these particles to be homogeneous spheres [1]. Nevertheless, most of the aerosol particles have irregular shapes and the scattering properties of that ones may differ quantitatively and even qualitatively from those of equivalent spheres in volume or surface area (i.e. Mie spheres). For these non-spherical particles, the T-Matrix method is one of the most powerful and widely used tools for computing electromagnetic scattering by single, homogeneous, arbitrarily shaped particles [3]. This technique is extremely mathematical and computationally intensive, and can require extensive effort just to define the size and shape of the particle, but has been proved to be more accurate than Mie theory.

2.1.1. Extinction, scattering and absorption coefficients.

When photons hit an aerosol particle, some will be scattered while others will be absorbed. Extinction is the sum of scattering and absorption.

The μ_{sca} and μ_{abs} describe the scatterance and absorptance, respectively, per unit distance in the medium.

$$\mu_i = N_0 \cdot \sigma_i \quad (1)$$

Where i may refer either to absorption or scattering, N_0 is the particle density of the medium and σ_i the optical cross section (e.g., σ_{sca} represents the area of the incident beam that becomes scattered light).

2.1.2. Extinction, scattering and absorption efficiencies.

The Q_{sca} and Q_{abs} are dimensionless efficiency parameters and describe what proportion of

the beam incident on a particle is diverted to scattering and absorption, respectively.

$$Q_i = \frac{\sigma_i}{\pi r^2} \quad (2)$$

Where πr^2 is the cross sectional area of a particle, projected onto a plane perpendicular to the direction of incident light. In case of irregular particles, r corresponds to the radius of equivalent spheres in volume or surface areas (i.e., Mie spheres).

2.1.3. Single scattering albedo.

The SSA for an aerosol layer is defined as the ratio between scattering and extinction by particle.

$$SSA = \frac{Q_{sca}}{Q_{ext}} = \frac{Q_{ext} - Q_{abs}}{Q_{ext}} = 1 - \frac{Q_{abs}}{Q_{ext}} \quad (3)$$

The SSA is a non-dimensional physical quantity and it is interpreted as the probability that a photon interacting with the particle will be scattered rather than absorbed. It takes values $0 \leq SSA \leq 1$; it is equal to 1 for nonabsorbing particles.

As an example, biomass burning containing a 100% of black carbon (BC) may have a SSA=0.3 if particles are assumed to be spherical, but a SSA around 0.19 if nonsphericity is taken into account [4].

2.1.4. Phase function and asymmetry parameter.

The phase function $P(\theta)$ describes the angular distribution of scattered energy and it is a non-dimensional physical quantity.

Regarding spherical particles, since the numerical phase function obtained from Mie calculations is extremely laborious to invert to get the angle of scattering (θ), the Henyey-Greenstein (HG) analytical phase function $P_{HG}(\theta, g)$ is widely used as a quite good approximation to the Mie phase function.

$$P_{HG}(\theta, g) = \frac{1 - g^2}{(1 + g^2 - 2g\cos\theta)^{3/2}} \quad (4)$$

Where g is the asymmetry parameter calculated using Mie theory and it is defined as the average cosine of the scattering angle of the scattered light. It is a non-dimensional physical quantity that for isotropic scatterers in a spherical geometry is written as:

$$g = \frac{1}{2} \int_{0^\circ}^{180^\circ} \cos\theta \cdot P(\theta) \cdot \sin\theta \cdot d\theta \quad (5)$$

It takes values $-1 \leq g \leq 1$; it is positive if the particle scatters more light toward the forward direction, is negative if more light is scattered toward the backward direction, and when the forward scattering is as much as the backward scattering, g becomes zero. In the atmosphere, monthly-mean aerosol g ranges from 0.6 to 0.82, having the largest particles the highest values (from AERONET data analysis) [4].

The phase function shows noticeable changes in the very narrow backscatter direction (i.e., $\theta > 150^\circ$), when considering different calculation methods (i.e., Mie, HG and T-matrix).

2.1.5. Aerosol size distribution.

As far as the size distribution of atmospheric aerosols is concerned, most of the scientific community agrees in a log-normal distribution.

$$\frac{dN}{dr} = \frac{N_0}{r\sqrt{2\pi\sigma^2}} \exp\left[\frac{-(\ln(r) - r_0)^2}{2\sigma^2}\right] \quad (6)$$

dN/dr is the particle density per radius interval, r_0 is the modal radius and σ the width of the mode (i.e. standard deviation). In case of irregular particles, r corresponds to the radius of equivalent spheres in volume or surface areas (i.e., Mie spheres).

Notwithstanding mono-modal log-normal size distributions may not be sufficient to describe any atmospheric size distribution adequately. In that case, distributions can be well approximated by multi-modal distributions, which are sums of several log-normal size distributions.

3. Methods and materials: simulations

This work has followed three steps; first, we have characterized our aerosol samples, second, we have calculate the aerosol optical properties using Mie theory, resulting in a collection of values depending on the size distribution, and third, radiometric results have been obtained from Monte Carlo simulations taking into consideration the aerosol optical parameters calculated before and the Henyey-Greenstein approximation.

It should be noted that some of the code used in this work was previously developed (Mie calculations and Monte Carlo method) by Maria Ballesta [\[5\]](#) in C++ using QT creator.

Regarding the aerosol size distribution, GNU Scientific Library (GSL) has been used to generate the log-normal distributions. GSL is a collection of routines for numerical computing in C, including functions for generating random number distributions [\[6\]](#). However, this library is not compatible with QT Creator, so instead, all calculations in this work have been adapted and developed in C++ using another software called Microsoft Visual Studio. Additionally, all the results have been plotted using Matlab.

3.1. Aerosols samples characterization

The parameters needed to characterize our samples and later on calculate their optical properties are; the size distribution, the index of refraction, the wavelength and the density particle. However, as it has been said before, every experiment is unique and not every paper shows the whole ensemble of parameters, so we have chosen our aerosol species from which the most information is available and we have selected a collection of data from the literature that is consistent, i.e. that corresponds to experiments conducted under similar conditions. Thus, as it has been said before, three different species of fog, biomass burning, and dust have been selected; in particular, radiation fog, pine wood burning, and transported desert dust (MITR). All three samples have been assumed to be fitted in a mono-modal log-normal size distribution.

Radiation fog is one of the most typically encountered in nature and it is generated by radiative cooling of an air mass when meteorological conditions are favorable, this means, very low speed winds, high relative humidity, clear sky, and low temperature. So this is a type of fog that generally appears during the night and at the end of the day, in winter, particularly in the valleys [7]. Regarding shape and composition, fog particles are widely assumed to be spherical and mainly consist of water, however they are formed from condensation nuclei of other aerosols, thus the refractive index depends on its chemical composition and can vary a lot. Notwithstanding, in large fog particles ($r > 1\mu m$), the amount of water is large enough and the use of the refractive index of water is usually justified.

Biomass burning, due to wildfires or the domestic use of wood fuel, releases the smallest particles into the atmosphere, and is one of the largest sources of organic aerosols, with as much as 30% of aerosol mass belonging to black carbon (BC), which is the largest absorbing sub-micron type of aerosol with an imaginary part of its refractive index up to 1.9 (in the visible) [8]. In terms of shape and size distribution, smoke particles are irregular, that is, nonspherical, and it has been observed that between 80 and 90% of the particles released by biomass burning are smaller than $r = 1\mu m$.

Mineral transported (MITR) aerosol or transported desert dust, it is used to describe the wind blown dust advected from the desert regions, transported over long distances, with a reduced amount of large particles (the lifetime in the atmosphere, before they hit the ground, of Sahara desert dust aerosols larger than $r = 20\mu m$ is of the order of 12h) [9]. Desert dust is one of the major constituents of natural aerosol particles in the atmosphere and the African Sahara is the largest desert area and also the primary dust source on Earth. In terms of shape and composition, dust aerosols are exclusively non-spherical, and consist of a complex mixture of various minerals, mainly clays, calcite, quartz, feldspars and iron oxides.

All selected data from the three species of aerosols have been gathered in table I.

Table 1: Log-normal parameters (r_0, σ), radius spectrum, wavelength dependent refractive index ($\tilde{n}(\lambda)$) and particle density (N_0), corresponding to our aerosol samples.

	Radiation fog	Biomass smoke	Transported dust
r_0	0.64 μm	6.49 nm	0.50 μm
σ	0.59	1.271	2.20
radius spectrum (μm)	0.01 - 15	0.01 - 1	0.02 - 5
$\tilde{n}(\lambda) = n + i\kappa$	1.3347 + i 3.7947·10 ⁻⁹	1.49 + i 0.013	1.53 + i 0.008
$\lambda(nm)$	550	675	550
N_0 (particles/cm ³)	10 ³	10 ⁴	10 ²

3.2. Calculation of the aerosol optical properties using Mie theory

A collection of optical parameters according to their size distribution, within the radius spectrum described in table I, and their corresponding weighted mean values have been calculated. In particular, 10⁴ different values have been calculated.

3.3. Montecarlo radiative transfer simulation of light scattering

$5 \cdot 10^4$ packets of photons with 100% initial energy are shot, in a transverse (z) direction, at the start of a cubic volume (x,y,z) containing the turbid medium. The dimensions of that volume have been chosen such that the energy transmitted through it ends up being almost 0%, meaning we have no visibility. In the particular case of fog we have not been able to generate such a large volume due to the computational capacity of the CPU.

4. Results and discussions

4.1. Size distribution

In figure 1, we present the corresponding uni-modal log-normal size distribution for our three species of aerosols according to the parameters described in table 1.

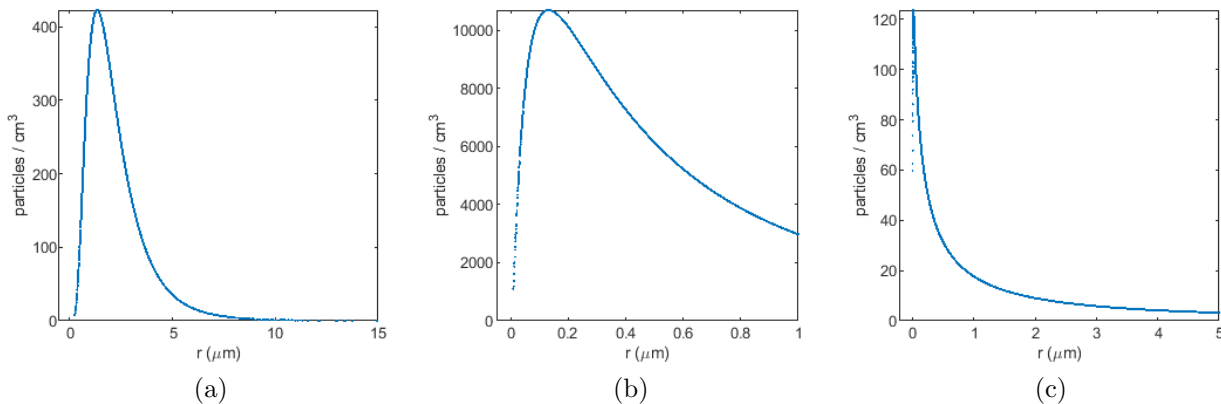


Figure 1: Log-normal size distributions. (a) radiation fog, (b) biomass burning, (c) transported desert dust.

4.2. Phase function

In figure 2, we present the phase function for three different sizes (radii) of our species of aerosol assuming spherical particles and using Mie theory and the Henyey-Greenstein approximation (4) for a hundred scattering angles between 0 and 180 degrees.

In broad terms, it is observed that all the scattering phase functions decrease with the increase of scattering angle. The main differences between Mie and HG phase functions are the lack of oscillations and the disappearance of the backscattering peak ($\theta > 150^\circ$) when using HG. If we compare our results with those from the literature we can assure that, in the case of fog (figure 2a vs. figure 3a), the results are more accurate using Mie theory rather than HG, however, in the case of biomass burning, assuming spherical particles, the conclusion is the opposite (figure 2b vs. figure 3b black line). And regarding dust particles, it can be observed that T-matrix method does not show the backscattering peak when non-spherical particles are assumed (figure 2c vs. figure 3c). It should be noted that any of the plots from the literature in figure 3 does not show oscillations because the curves have been smoothed by superposition of all the results obtained for the different sizes in the log-normal size distribution.

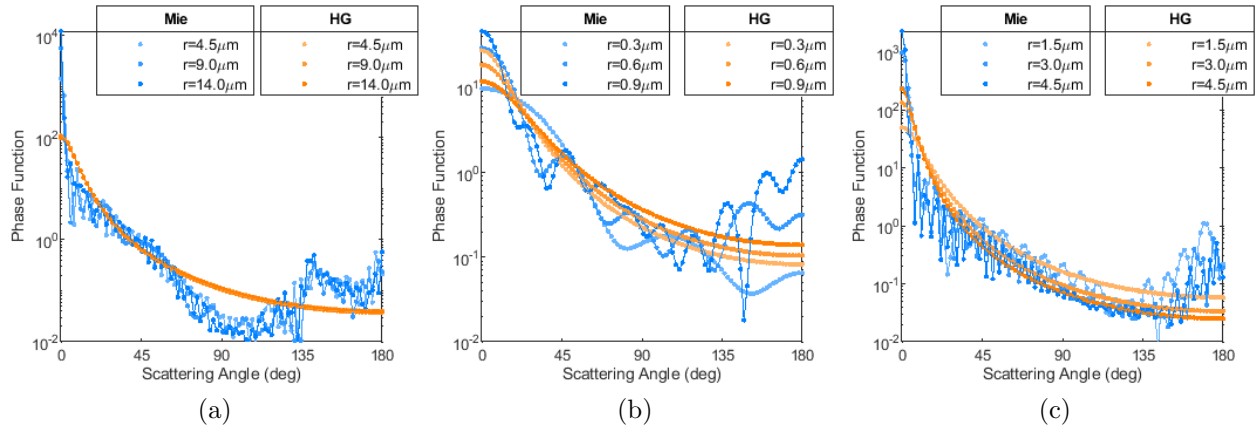


Figure 2: Mie (blue) and HG (orange) phase functions versus scattering angle for three different sizes (radii in the legends) of spherical particles and a hundred scattering angles between 0 and 180 degrees. (a) radiation fog, (b) biomass burning, (c) transported desert dust.

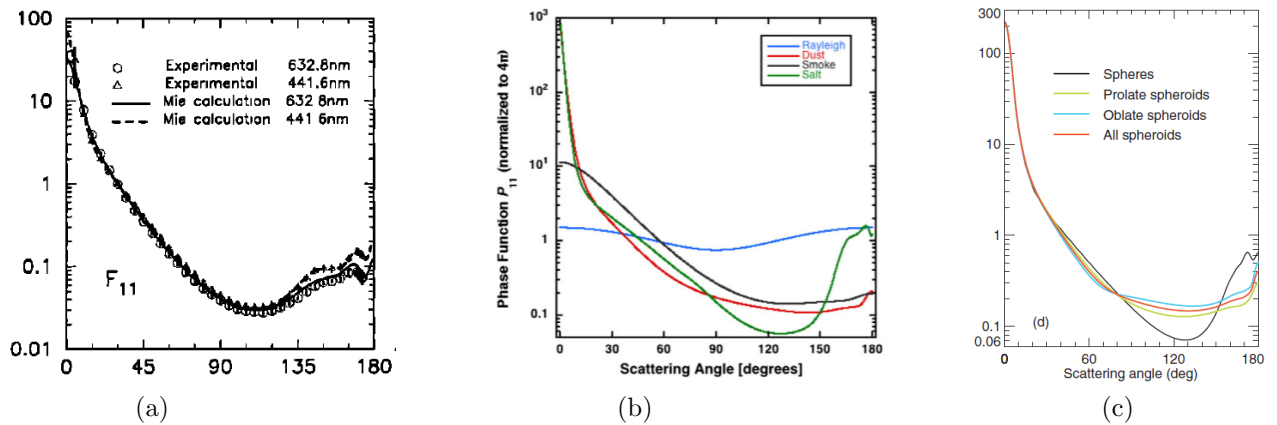


Figure 3: Phase functions versus scattering angle for simulations and experiments under similar conditions. (a) Mie phase functions and experimental results for water droplets (figure 4 in [10]), (b) Mie phase functions for smoke (black) and dust (red) (figure 3.1 in [11]), (c) T-matrix phase functions for dust (plate 2.3d in [3]).

4.3. Asymmetry parameter and single scattering albedo

In figure 4, we present the results for the asymmetry parameter and single scattering albedo corresponding to our three species of aerosols.

Weighted mean values of g and SSA according to the log-normal size distribution have been calculated as well; $\bar{g} = 0.8698, 0.6516, 0.8681$, and $\text{SSA} = 1.0000, 0.7785, 0.6583$, for radiation fog, biomass burning, and transported desert dust, respectively.

The asymmetry parameter is always positive for the three samples, that is, particles scatter more light toward the forward direction than toward the backward direction. As regards the weighted mean values, it is noticeable that fog and dust have similar values while smoke has a smaller value and therefore scatters less light toward the forward direction compared to the other two. Furthermore, it can be seen that the largest particles have the highest and more stable values, and \bar{g} values agree quite well with the range of values established by AERONET for monthly-mean aerosol asymmetry parameter in the atmosphere (0.6 to 0.82).

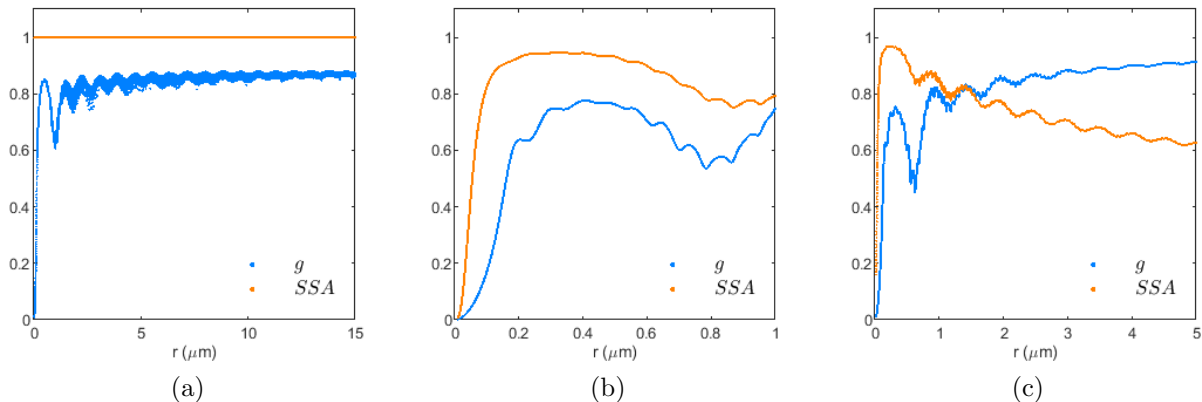


Figure 4: Asymmetry parameter. (a) radiation fog, (b) biomass burning, (c) transported desert dust.

Regarding the single scattering albedo, it can be observed that radiation fog is a non-absorbing medium since $SSA=1$, as it is expected according to its imaginary part of the refractive index (near to zero, table [1](#)). Thus, the decrease in visibility during fog episodes is basically due to light scattering and not absorption. On the other hand, smoke and dust have a more variable SSA, always smaller than 1, depending on the particle size, showing a combination of absorbing and scattering properties in the medium. In addition to this, it is clearly seen, especially for dust, that SSA has a trend to decrease with increasing particle size. According to the imaginary part of the refractive indices of biomass burning and transported desert dust (0.013 and 0.008, respectively, see table [1](#)), we may expect smoke to have a larger absorption efficiency than dust, albeit, if we take a look at the weighted average scattering and absorption efficiency values, it seems that dust is more absorbing than smoke, and in turn smoke is more scattering than dust ($Q_{sca} = 1.6824$, $Q_{abs} = 0.4716$, for biomass burning, and $Q_{sca} = 1.5389$, $Q_{abs} = 0.6666$, for transported desert dust). This fact illustrates the relevance of the size distribution in the subsequent radiometric calculation.

4.4. Radiative transfer

Montecarlo radiative transfer simulations have been implemented taking into account the weighted mean values of aerosol optical parameters calculated before using Mie theory (except for g , which is the only parameter susceptible to be applied specifically at each particle depending on its size) and Henyey-Greenstein approximation.

In figure [5](#), we present the percentage of energy transmitted and reflected along the turbid media in z distance. Two approaches have been considered; using the weighted mean value of the asymmetry parameter \bar{g} and the actual g value at each particle depending on its size $g(r)$. Furthermore, transmitted energy has been fitted to a negative exponential ($a \cdot e^{-bz}$) in order to get the resemblance with the Beer-Lambert law ($I(z) = I_0 \cdot e^{-\mu_{ext}z}$) and reflected energy has been fitted to a smoothing curve.

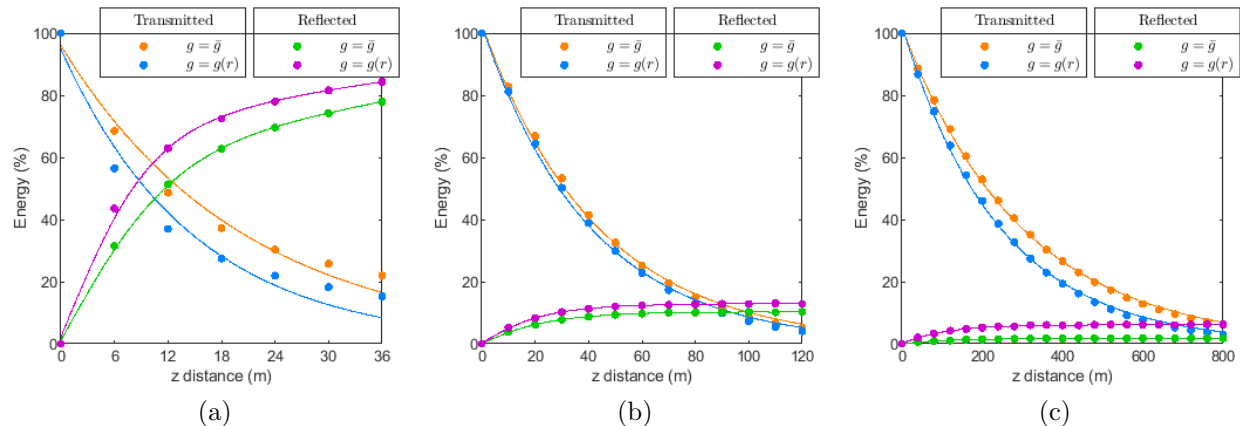


Figure 5: Percentage of transmitted (orange and blue) and reflected energy (green and purple) taking into account the weighted mean value of g (orange and green) and the specific value for each particle according to its size (blue and purple). Transmitted energy has been fitted to a negative exponential ($a \cdot e^{-bz}$) and reflected energy to a smoothing curve. (a) radiation fog, (b) biomass burning, (c) transported desert dust.

Since we are simulating propagation of light through an aerosol volume or layer, SSA (and the rest of parameters derived from it, such as μ_i and Q_i) is commonly defined as a global value for the whole ensemble (i.e., the weighted mean value obtained before) and it is applied to each individual particle found along the Monte Carlo simulation, that is, at each step. However, the phase function is a single scattering property and consequently g may be treated as that as well. Thus both results, \bar{g} and $g(r)$, have been plotted in figure 5 and the differences have been discussed to consider whether the computation of $g(r)$ at each particle is worth. Fog has the largest discrepancy, about 12%, smoke less than 3% and dust less than 8%, in both transmitted and reflected energy, so it depends on the level of accuracy required to decide whether to choose the use of one parameter or the other.

As far as Beer-Lambert law is concerned, it can be seen from figure 5 that the negative exponential fits perfectly with the energy transmitted through the volume in absorbing media (i.e., smoke and dust), but it does not fit so well to the results obtained for a non-absorbing medium (i.e., fog). The negative exponents corresponding to $g(r)$ fitted curves are $b = 0.0674$, 0.0248 and 0.0041 m^{-1} , for fog, smoke and dust, respectively, and the extinction coefficients from Mie calculations are $\mu_{ext} = 1.3312$, 0.0563 and 0.0081 m^{-1} , respectively. As it can be seen, the values does not coincide, in particular, it seems to be around a factor of 2 that sets them apart. However, it should be noted that the energy we plotted corresponds to the total energy in the xy -plane of the cubic volume $xyz = z^3$, which is a different area at each distance z , while the extinction coefficients from Beer-Lambert law are calculated on the same area at different distances (z).

Finally, from transmitted and reflected energy it is observed that most of the energy lost is reflected back, meaning no absorption, in the case of fog, while for smoke and dust, most of the energy is lost inside the medium by absorption (the energy reflected back is less than 10%). In terms of visibility, it is clear to see that dense radiation fog is the medium with the worst visibility of all, with up to 20% of initial transmitted energy at 36 metres distance, followed by biomass burning and transported desert dust, with up to 5% of initial transmitted

energy at 120 metres and 800 metres distance, respectively.

5. Conclusions and future work

In this work we have been interested in using, modifying and adapting an existing radiometric model in order to simulate propagation of light in radiation fog, biomass burning and transported desert dust, as a progress towards a model for the propagation of light in turbid media with irregular particles. The existing code has been improved and adapted from QT Creator to Microsoft Visual Studio (C++) and all the results have been plotted using Matlab. A very extensive literature search has been necessary in order to properly characterize the chosen aerosol samples and to understand which are the most suitable methods to simulate scattering in this kind of turbid media.

A remarkable difference has been observed in the radiometric model between absorbing and non-absorbing media, where Beer-Lambert law does not fit as well.

For future work, taking into account the above mentioned, it would be interesting to validate the model experimentally as well as implement a new method of scattering calculations able to reproduce properly the scattering properties of irregular particles (e.g., T-matrix method), which was not possible to implement due to the limited time available for the development of this MSc Thesis, and compare it with Mie results. Furthermore, to extend this simulation, it will be useful to characterize new samples of aerosols.

References

- [1] Shettle E P 1990 Models of aerosols, clouds, and precipitation for atmospheric propagation studies *AGARD (Advisory Group for Aerospace Research & Development)*
- [2] Hess M, Koepke P and Schult I 1998 Optical Properties of Aerosols and Clouds: The Software Package OPAC *Bulletin of the American Meteorological Society* **79,5**
- [3] Mischenko M I, Hovenier J W and Travis L D 2000 Light Scattering by Nonspherical Particles (San Diego, California: Academic Press)
- [4] <https://www.intechopen.com/chapters/38765>
- [5] Ballesta Garcia M 2018 Long-range polarimetric propagation in turbid media (MSc thesis)
- [6] <https://www.gnu.org/software/gsl/doc/html/index.html>
- [7] Muhammad S S, Flecker B, Leitgeb E and Gebhart M 2007 Characterization of fog attenuation in terrestrial free space optical links *Optical Engineering* **46,6**
- [8] Sarpong E, Smith D, Pokhrel R, Fiddler M and Bililign S 2020 Refractive Indices of Biomass Burning Aerosols Obtained from African Biomass Fuels Using RDG Approximation *Atmosphere* **11,62**
- [9] Mahowald N, Albani S, Kok J F, Engelstaeder S, Scanza R, Ward D S and Flanner M G 2014 The size distribution of desert dust aerosols and its impact on the Earth system *Aeolian Research* **15** 53-71
- [10] Volten H, Muñoz O, Rol E, de Haan J F, Vassen W, Hovenier J W, Muinonen K and Nousiainen T 2001 Scattering matrices of mineral aerosol particles at 441.6 nm and 632.8 nm *Journal of Geophysical Research* **106,D15** 17375-17401
- [11] Kokhanovsky A A, Davis A B, Cairns B, Dubovik O, Hasekame O P, Sano I, Mukai S, Rozanov V V, Litvinov P, Lapyonokd T, Kolomiets I S, Oberemok Y A, Savenkov S, Martinc W, Wasilewski A, Di Noia A, Stap F A, Rietjens J, Xub F, Natraj V, Duanj M, Cheng T and Munroa R 2015 Space-based remote sensing of atmospheric aerosols: The multi-angle spectro-polarimetric frontier *Earth-Science Reviews* **145** 85-116